A LOW TEMPERATURE PHOSPHORESCENCE DETECTOR FOR GAS CHROMATOGRAPHY

By

NANCY JEAN MULLINS

A DISSERTATION PRESENTED TO THE GRADUATE SCHOOL
OF THE UNIVERSITY OF FLORIDA IN PARTIAL FULFILLMENT
OF THE REQUIREMENTS FOR THE DEGREE OF
DOCTOR OF PHILOSOPHY

UNIVERSITY OF FLORIDA

1994

ACKNOWLEDGEMENTS

None of this work could have been done without the guidance wisdom, and support of Dr J D Winefordner It has been a truly wonderful opportunity for which I am grateful To my parents, I owe everything, they have supported and believed in me unconditionally I can never repay my family for their understanding and generosity--I love them all very much Special acknowledgement must go to Barclay for making each day bearable.

There have been many people who have made this experience less painful than it could have been, and I thank them for being my friends. Brad Jones, Lynn Perry, Ramee Indralingam, Gail Beals, Greg Mead, Cecilia Basic Freund, Mike Freund, Irene Poyer, Stefanie Pagano MaryAnn Gamshefski Donna Robie, Andi Pless, Nicki Schnitz, John Clos, Martha Dunaway, Kelly Shea, and especially Monica Escobar, without whom I never could have survived the final year There were many wonderful people at Southwest United Methodist Church whose prayers and assistance were always with me the Van Arnams, the Williams, the Bateys, the Moyes, and Reverend Ann and Dave Hutchens. May God bless them all

I would like to thank all of the gentlemen in the machine shop, Chester Eastman, Dailey Burch, Vern Cook, and Jerry Holland They have always gone the extra mile to get me what I asked, and to answer my questions The ladies in

purchasing, especially Bev Lisk, worked hard to make sure that needed equipment was ordered as quickly as possible. Two very special secretaries, Jeanne Karably and Susan Ciccarone, were always available to answer my questions and to solve my problems. Without these people, this work would have been nearly impossible. They are truly professional, and the best of the best.

Finally, I would like to thank BP Oil Company for awarding me the fellowship supporting my research, especially George Havrilla, who was supportive in all phases of my work.

TABLE OF CONTENTS

ACKNOWLEDGMENT ii

LIST OF TABLES vi

LIST OF FIGURES vii

ABSTRACT xi

CHAPTERS

1 LOW TEMPERATURE MOLECULAR LUMINESCENCE SPECTROSCOPY 1

- Introduction 1
- Band Broadening Mechanisms in Molecular Spectroscopy 6
- Supersonic Jet Expansion 12
- Matrix Isolation 16
- Shpol'skii Spectroscopy 17
- Site Selection Spectroscopy 21
- Previous Work 21
- Focus of This Work 23

2 LOW PRESSURE OUTLET GAS CHROMATOGRAPHY 26

- Introduction 26
- Band Broadening in Chromatography 32
- Analysis Time 36
- Effects of Vacuum Outlet Conditions on This Work 40

3 EXPERIMENTAL PROTOCOL AND INSTRUMENTATION 42

- Spectroscopy 42
- Vacuum Chamber 44
- Chromatography 46
- Evolution of the Transfer Line Design 46
- Matrix Isolation 54
- Shpol'skii Matrices 54
- Reagents 56
- Procedure 58

4 RESULTS AND DISCUSSION 60

5 CONCLUSIONS AND FUTURE WORK 99

Conclusions 99
Future Work 103

REFERENCES 106

BIOGRAPHICAL SKETCH 110

LIST OF TABLES

Table
1 Comparison of Low Temperature Techniques 25

2 Definitions of Chromatographic Parameters and Symbols Used in This Chapter 27

3 Reagents 58

4 Retention Times of Test Compounds (in Minutes) under Atmospheric and Vacuum Outlet Conditions 64

LIST OF FIGURES

Figure

1.1 Jablonski Diagram showing the energetic processes in molecular luminescence spectroscopy . . . 7

1.2 The orientation sites of a molecule in a crystalline matrix result in different crystal field interactions with the analyte guest. Each different site is designated by a greek letter. This figure shows some possible orientations, relative to the crystal field, designated σ . . . 9

1.3 Transition linewidths in a crystalline matrix a) single vibronic transition showing the zero phonon line and phonon wing, b) closely spaced transitions and their resulting linewidth contributions . . . 11

1.4 Supersonic Jet Diagram. R designates the sample reservoir, X_1 designates the free flow regime, and X_m designates the mach zone . . . 13

1.5 Simplified supersonic jet nozzles. a) simple expansion nozzle, b) sheath flow nozzle . . . 15

1.6 Relationship of solvent shape and dimensions to molecule dimensions. Length and geometry are both considerations. Shown here are some molecules and their optimal solvents . . . 18

1.7 Effect of the rate of cooling on sample homogeneity. As is seen, the number of sites is larger if the crystal is cooled too quickly . . . 19

1.8 Solvent effect on the observed fluorescence emission spectra of 7 methoxybenzo[a]pyrene. a) the top spectrum is 5 ppb in n-octane b) the bottom spectrum is 500 pptr in n-decane Note that the observed transitions are not at the same wavelengths and that the intensity is greatly affected 20

1.9 Site selection spectra of 11 methylbenz[a]anthracene in n-octane. Three sites are present if non-selective excitation is used. The effect on the observed fluorescence spectra is seen when the three sites are selectively excited The spectra on the left are excitation spectra, those on the right are of fluorescence emission The fluorescence linewidths are noticeably narrower, and the spectra are far less congested 22

2.1 Determination of the FWHM value from a Gaussian chromatogram peak 31

2.2 Golay curves on short columns at four different outlet pressures Note that the difference between the 100 torr and 0.1 torr curve is minimal This suggests that pressures below this value will exhibit no further improvement in analysis time This data is for a 4 m column 34

2.3 Golay curve for 2 lengths of column at two different outlet pressures It is clearly seen that the long column experiences far less vacuum effect than a short column Note that the optimum linear velocity is shifted to a higher value in both the long and short columns 38

3.1 Top view of chamber and optical configuration 43

3.2 Side view of vacuum chamber 45

3.3 Interface design for the first phase of this work 47

3.4 Dual capillary interface design for the second phase of this work 51

3.5 Bulkhead interface design for the third phase of this work. The stainless steel union extends 1 m from the interface to the GC, it is not shown to scale. 53

3.6 Hexane reservoir for dual capillary matrix isolation 55

3.7 Saturation pressure curve for hexane 57

4.1 Background signal of LTMLS detector at the start of this work 61

4.2 Background spectrum taken after renovating the vacuum system and removing the molecular beam valve. 63

4.3 Phosphorescence matrix isolation spectrum of 67.5 ppm fluorene, background corrected, in 3% argon carrier gas. The sample mass was 0.34 μg. The primary feature of the spectrum is the delayed fluorescence peak on the left, and fine structure is absent. 65

4.4 Flow rate calibration curve for needle valve control of gas tank. The regulated tank pressure was 6 psi. The first needle valve was open to a set position 67

4.5 Matrix isolation luminescence spectrum for 67.5 ppm fluorene in argon. The sample mass was 0.34 μg, and the argon flow was 0.5 mL/min 69

4.6 Matrix isolation luminescence spectrum for 81.5 ppm triphenylene in argon. The sample mass was 0.41 μg, and the argon flow was 0.5 mL/min 70

4.7 Matrix isolation luminescence spectrum for 131 ppm 1,2 benzofluorene in argon. The sample mass was 0.65 μg, and the argon flow was 0.5 mL/min 71

4.8 Matrix isolation luminescence spectrum for 114 ppm 2 3-benzofluorene in argon. The sample mass was 0.57 μg, and the argon flow was 0.5 mL/min 72

4.9 Matrix isolation luminescence spectrum for 65.5 ppm phenanthrene in argon. The sample mass was 5 μl, and the argon flow was 0.5mL/min. 73

4.10 Phosphorescence spectrum for 67.5 ppm fluorene deposited onto hexane. The sample mass was 0.34 μg, and the spectrum was corrected for background 74

4.11 Matrix isolation phosphorescence spectrum for fluorene in argon, corrected for background. The argon flow was 0.5 mL/min and the sample mass a) 0.006 μg, b) 0.02 μg, c) 0.07 μg, d) 0.10 μg, e) 0.34μg f) 0.41 μg 76

4.12 Matrix isolation phosphorescence and delayed fluorescence spectra of the 20.25 ppm fluorene standard as a chromatographic peak develops. The sample mass was 0.10 μg and the time span 5.5-7.5 min, at 0.4 min intervals 83

4.13 Shpol'skii luminescence spectra of 70 ppm standard mixture. Sample mass was 0.35 μg, and the time span shown, at 0.5 minute intervals a) 3-16 min, b) 16-29 min, c) 29-40 min 84

4.14 Luminescence spectra of 65.5 ppm phenanthrene standard in different matrices a) 0.33 μg sample in argon, b) 0.13 μg sample in hexane 88

4.15 Chromatogram of five-component mixture scanned at 340 nm. The top spectrum is for the entire range; the bottom spectrum is for the time after fluorene has eluted 89

4.16 Chromatogram of five-component mixture scanned at 360 nm. The top spectrum is for the entire range; the bottom spectrum is for the time after fluorene has eluted 90

4.17 Chromatogram of five-component mixture scanned at 500 nm. The top spectrum is for the entire range, the bottom spectrum is for the time after fluorene has eluted 91

4.18 Delayed fluorescence spectrum of triphenylene in EPA at 77K shown at left, phosphorescence shown to the right 94

4.19 Delayed fluorescence spectrum of phenanthrene in EPA at 77K shown at left, phosphorescence shown to the right 95

4.20 Fluorescence spectrum of 2,3-Benzofluorene 96

4.21 Delayed fluorescence spectrum of fluorene in EPA at 77K shown at left phosphorescence shown to the right. 97

Abstract of Dissertation Presented to the Graduate School
of the University of Florida in Partial Fulfillment of the
Requirements for the Degree of Doctor of Philosophy

A LOW TEMPERATURE PHOSPHORESCENCE DETECTOR FOR GAS CHROMATOGRAPHY

By

Nancy Jean Mullins

April 1994

Chairperson: James D. Winefordner
Major Department: Chemistry

Low temperature molecular luminescence spectroscopy (LTMLS) techniques are important due to their ability to differentiate compounds having very similar structures. If the analyte is frozen in a select matrix, the resolution and sensitivity of LTMLS is very high. LTMLS is a logical choice as a detection method for separation techniques because the resolution of the separation technique is coupled with the spectral resolution achieved by the detector. Such work has been performed with fractions from liquid chromatography (LC), and with eluent from gas chromatography (GC).

Until now, such detectors have been cumbersome, able to sample for a period of time, but requiring a warm-up period to clean the sample cell. A self-cleaning phosphorescence detector, created in our lab, was capable of sampling continuously,

but was plagued with high background signal. Additionally, choice of matrices was limited to gases or gaseous solutions.

In this work, the LTMLS system was improved: eliminating the background signal, enhancing spectral resolution, and increasing potential sensitivity. The moving belt, which collected the sample and positioned it for the optical system, was modified to allow a gear driver. Belt slippage was eliminated, and reproducible speeds were ensured.

The focus of the work was to create a dual capillary transfer line, enabling the eluent from the GC to be co-deposited and frozen with the matrix of choice. In this way, the analyte need not be soluble in the matrix, and the separation remained unaffected by the addition of the matrix. Because the amount of a component in a gaseous solution is limited by its vapor pressure, optimal amounts of a given matrix may not be easily obtained. A solvent reservoir was then designed which extended the range of matrices to less volatile substances. The reservoir was a stainless steel cylinder with high pressure fittings in which the desired volatile liquid was heated. Vapors were controlled by a low pressure regulator and needle valve which were calibrated for the desired flow. The results from this portion of the work demonstrated the utility of such a reservoir, which is inexpensive, simple in design, and versatile.

CHAPTER 1
LOW TEMPERATURE MOLECULAR LUMINESCENCE SPECTROSCOPY

Introduction

Cooling molecules to cryogenic temperatures has long been known as a means of enhancing their luminescence spectral resolution [1]. In general, the bands are narrower and signals higher than those obtained under room temperature conditions. Low temperatures alone, however, do not afford the fine spectral resolution sometimes seen. Environmental factors also contribute to the bandwidth of molecular luminescence spectra. Those spectra taken when the molecules of interest are isolated from one another have significantly narrower bandwidths due to decreased energy transfer mechanisms. Several techniques which utilize this concept are frequently used: supersonic jet expansion, matrix isolation, and Shpol'skii spectroscopy. Each of these techniques will be addressed and Table 1 is a comparison of the techniques.

Before broadening mechanisms are discussed, a brief discussion of the phenomenon of luminescence will be introduced. Figure 1.1 is a Jablonski diagram, adapted from Ingle and Crouch [2], in which the energetic processes of luminescence are described. In a neutral aromatic molecule, the ground state is a singlet state. According to the selection rules, absorption of energy must result in a transition between electronic states of the same multiplicity ($S_0 \rightarrow S_n$) and between vibrational states whose vibrational quantum numbers, v, differ by 0, or by integral values. The

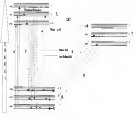

Figure 1.1 Jablonski Diagram showing the energetic processes in molecular luminescence spectroscopy (Taken from Reference 2)

rate at which radiation is absorbed is dependent on the molar absorptivity of the compound, and for aromatic compounds, the absorption time is on the order of 10^{-14} to 10^{-15}s [2]

Just as the molecule has defined routes of absorption of energy, it also has defined radiative decay parameters The favored route of decay is that which minimizes the lifetime of the excited state Thus, the process with the more favorable rate constant is often the observed process [3] Vibrational relaxation is defined as the loss of energy within an electronic state as the excited vibrational levels lose energy through thermal or vibrational motion In solutions, this process continues through many collisions until the electron moves to the lowest vibrational level of the electronic state. In gas phase or crystalline matrices, however, this relaxation may not completely depopulate the higher vibrational levels of the excited state due to decreased collision frequency Thus, while only transitions from the $v''=0$ state may be observed for solution samples, other transitions may be observed in the gas phase or in crystalline matrices

Fluorescence is defined as the transition from a vibrational level of the excited state (S_1) to any of the vibrational levels of the ground state (S_0) From these allowed processes, only clearly defined wavelengths should be seen from a given molecule As noted before, selection rules also state that transitions may only occur between electronic states of the same multiplicity Thus, a triplet to singlet transition, or vice versa, is forbidden A spin-orbit mechanism is one in which the angular momentum of an electron's spin is flipped resulting in some triplet character of the excited singlet state, and the excited triplet state created has some singlet state character. This process is termed singlet-triplet mixing. In this way, a process termed "intersystem crossing" occurs, whereby the triplet state may be populated.

Phosphorescence is defined as the transition from a vibrational level of the triplet state (T) to any of the vibrational levels of the ground state (S_0). As this transition is also forbidden, the lifetime of the transition (10^{-4} to 10^{4} s) is substantially longer than that of either the singlet excited state, fluorescence (10^{-10} to 10^{-6} s), or vibrational relaxation (10^{-11} to 10^{-13} s). Because energy is lost in the vibrational relaxation of the excited states, the luminescence emission is shifted to longer wavelengths than those of the excitation spectrum [2].

In room temperature solutions, phosphorescence rarely occurs. This is due to the long lifetime of the triplet state, which has an increased probability of collisional transfer of energy to solvent and impurity molecules, compared to that of the competing processes [4]. Procedures which reduce the collisional deactivation include freezing the sample solution, or placing the sample on a solid substrate such as filter paper or TLC plates [5,6,7]. Room temperature solution phosphorescence may also be observed if heavy atoms are introduced into the solution [8], if a micellar solution of the analyte is made [9], or in sensitized phosphorescence in which the analyte's T_1 energy is transferred to an acceptor molecule, which then phosphoresces. Suitable acceptor molecules are 1,2-dibromonaphthalene and biacetyl [4].

Scattering processes may also take place in molecules interacting with the excitation radiation. If the scattering is elastic, the scattered radiation has the same energy as the incident light this process is known as Rayleigh scattering If the emitted radiation is inelastic, meaning that its energy differs from that of the excitation source Raman scattering is seen If the molecule is excited to a virtual energy level (one whose energy lies just below an electronic state), nonresonance Raman scattering can occur If the emission radiation is of higher energy than the absorbed radiation, this is termed a Stokes transition If the emitted radiation is less energetic than the excitation radiation, this is termed "anti-Stokes" transition Resonance Raman is a technique in which the molecule is excited to an energy level very close to that of an electronic absorption band The emitted radiation is a direct transition from the v'' state to a v' state, which occurs without vibrational relaxation The resonance Raman emission is immediate compared to the much slower fluorescence with a nanosecond lifetime, and can be distinguished from fluorescence by signal development and decay time using a pulsed laser Additionally, Raman can be observed with the excitation slightly above or below that of the vibrational level, in near resonance Raman, while fluorescence cannot. The cross section of a Raman transition is very small compared to fluorescence, usually the Raman signal is not detectable in the presence of a fluorescence signal [2]

Although electronic transitions are defined, it is possible that the observed spectrum differs from what is expected Factors which influence the observed spectrum include environmental influences, such as a magnetic fields, solvent effects, electric fields, or energy transfer mechanisms These effects are usually termed band broadening mechanisms in that the expected transition is actually expressed as a combination of transitional lines [1]

Band Broadening Mechanisms in Molecular Spectroscopy

Homogeneous broadening mechanisms are those processes common to all molecules of the same type in a sample. This broadening may be due to deactivation of populated excited states by collision or may be due to the simultaneous excitation of multiple vibrational or rotational levels of a given molecule. These mechanisms are independent of environmental conditions other than temperature.

As the temperature is lowered, the number of collisions decreases, so that the lifetime of the excited state of the molecule is increased. The relationship of linewidth, $\Delta\nu$, to transition lifetime, τ, is described by Heisenberg [2] as

$$\tau\Delta\nu > \frac{1}{2\pi c} \tag{1.1}$$

where τ is in s, c is the speed of light in cm s^{-1}, and $\Delta\nu$ is in cm^{-1}. Because the lifetime is uncertain, the spectral linewidth is a distribution. The term given to the broadening due to this uncertainty is "natural broadening." Another implication of this relationship is that if an excited state is long-lived, it will have a narrow transition linewidth [1].

Another type of broadening relates to the close spacing of the vibrational levels of molecules. A simple description of this is given using the harmonic oscillator model, where ΔE_v is the energy gap defined by the vibrational transition (cm^{-1}), where $\hbar$ is Planck's constant divided by 2π (Js), where k is the oscillator force

$$\Delta E_v = \frac{h}{c}\sqrt{\frac{k}{\mu}}(v_2 - v_1) \qquad (1.2)$$

constant (dyne cm^{-1}), μ is the reduced mass of the groups involved in the vibration (g), and v is the vibrational quantum number For the larger molecules studied in this work, the reduced mass is large, hence the energy gap is small. Because these vibrational levels are closely spaced, several may be populated by the excitation source Each populated vibronic state contributes a line to the spectrum. The observed linewidths may be a single transition, or appear as an unresolved smeared sum of the contributions which leads to broadening of the apparent emission linewidth [10].

Similarly, the rotational contribution to broadening can be described using the rigid rotor model for molecules as where ΔE_j is the energy gap (J)

$$\Delta E_J = \frac{\hbar^2}{2I}[J_1(J_1+1) - J_2(J_2+1)] \qquad (1.3)$$

between the rotational levels described by J, the rotational quantum number, , and I the moment of inertia (kgm^2)

Further, the moment of inertia can be described as

$$I = \sum m_i r_i^2 \qquad (1.4)$$

where m_i is the mass of the *ith* atom in the molecule (g), and r_i the distance of the *ith* atom from the axis of rotation Again, for the large molecules investigated, these energy levels are very closely spaced allowing multiple levels to be populated. The rotational energy gap is much smaller than that for vibrational levels, however, and it is more likely to contribute to the observed homogeneous broadening. Whatever the source of homogeneous broadening, these mechanisms can be diminished to a negligible level at low temperatures, making low temperature techniques desirable.

Inhomogeneous broadening effects arise from variations in the electrical, magnetic, and solvent environment of each molecule. Each environmental effect has the capability of shifting the frequency of the transition of the emitted line. The linewidth of a transition is limited to the natural lifetime of the excited state, which cannot be changed. For this reason, the environment of each molecule or "microenvironment" is an important parameter in establishing experimental conditions. Inhomogeneous broadening may also arise from the excitation of molecules in different sites of the matrix. A site is a particular orientation of a molecule in its environment. Figure 1.2 shows some possible orientations of an analyte molecule in the crystal. A given transition has its own associated linewidth. If multiple sites of the analyte molecule are excited, they all contribute their associated linewidths. Again, the resulting band is the sum of all of the site contributions, leading to a broad band.

The extent of the observed broadening is largely dependent on the phase of the sample. In gaseous samples, often the temperature is elevated, so homogeneous broadening is significant. Another common form of band broadening seen in the gas phase is Doppler broadening. Doppler broadening is an apparent broadening of a

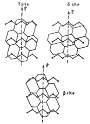

Figure 1.2 The orientation sites of a molecule in a crystalline matrix results in different crystal field interactions with the analyte guest. Each different site is designated by a greek letter. This figure shows some possible orientations, relative to the crystal field, designated $\vec{z}$. (Taken from Reference 1)

spectral line due to motion of the molecules relative to the detector. If the molecule is moving toward the detector, it appears to have a higher frequency than it actually has. If it is moving away from the detector, it appears to have a lower frequency. In liquid solutions, broadening is primarily inhomogeneous due to the rapidly varying interactions of analyte molecules with the solvent [11]. These effects cannot be reduced because the environment changes faster than the lifetime of the excited state [12].

In condensed phase samples, inhomogeneous broadening effects may predominate over pressure broadening effects, and bands in solution may be broader than can be attributed to collisional broadening. In the gas phase, this effect is seen in the broadened natural linewidths. A special case occurs with samples in a crystalline matrix. In this environment, interaction of the analyte, source, or of the emission with the crystal lattice gives rise to lattice vibrations, resulting in a wing on the transition linewidth, called a phonon wing. The vibronic transition line in this environment is termed the zero phonon line, or ZPL, designating a transition in which no lattice vibration (phonon) is created or destroyed in the matrix [13]. Although a zero phonon transition has a defined energy, interaction of the molecule with the matrix may lead to a difference in the energy of the observed ZPL and that of the natural or matrix-free transition. Figure 1.3 shows the effect that the phonon wings of closely spaced transitions can have on the observed spectra.

One means of comparing spectral resolution in low temperature molecular solids is to compare the Debye-Waller factor, α, defined as

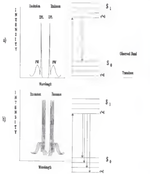

Figure 1.3 Transition linewidths in a crystalline matrix: a) single vibronic transition showing the zero phonon line and phonon wing b) closely spaced transitions and their resulting linewidth contributions

$$\alpha = \frac{I_{ZPL}}{I_{ZPL}+I_{PW}} \tag{1.5}$$

where I_{ZPL} is the intensity of the zero phonon line and I_{PW} is the intensity of the phonon wing. The higher the Debye Waller factor as α approaches the value of one, the less coupling that occurs between the electron transitions and the crystal lattice vibrations [14].

Finally, low temperature techniques are desirable because they allow the reduction of the number of possible sites. Fewer sites means that the excitation energy is less dispersed. each receives a greater proportion of the energy absorbed by the molecule. Each site which is able to absorb the excitation energy yields higher intensity spectral lines than in a less ordered medium.

Supersonic Jet Expansion

When a quantity of gas in a reservoir at high pressure is allowed to expand through an orifice into a region of low pressure, a high degree of cooling occurs. This effect is known as supersonic jet expansion and an excellent review of the technique in analytical methodology has been published [15]. The characteristic of supersonic jet expansion is a highly directional flow which occurs because of the high number of collisions in the high pressure region and in the nozzle. The directed flow has the property of a narrow velocity distribution which is shifted to higher flow velocity as the thermal energy of the sample is converted to kinetic energy. A consequence of the directed flow is a very high density of molecules along the axis of expansion which is thermally protected from the environment of the chamber by a

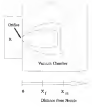

Figure 1 4 Supersonic Jet Diagram R designates the sample reservoir, X_f designates the free flow regime, and X_m designates the mach zone (Adapted from Reference 15) shock wave created by the expansion. A diagram of a supersonic expansion is given in Figure 1-4, adapted from Hayes and Small [15].

In this diagram, R is the reservoir region. As the gas passes from the reservoir into the chamber, three areas are defined by their axial distances from the orifice. The distance designated X_f in the diagram is the distance at which the frequency of collisions is zero. This is the start of the free molecular flow regime where the molecules are rotationally and vibrationally cooled, and at which they are free from matrix and are isolated. Another region is defined as the Mach disc, at distance X_m from the nozzle. This is the distance from the nozzle at which the shock wave ends. The shock wave acts to protect the molecular beam from collision with warmer molecules in the expansion chamber.

The sampling region is past X_f and is in the inner region of the diagram where the density of molecules is greatest and where they are thermally isolated. Despite the region being fairly high in density a high degree of dilution is inherent in expansion. One means of making the sampling region more focussed is to use a sheath gas. This technique increases the sampling number density and adds flow so that the technique can be coupled to low flow techniques, such as supercritical fluid chromatography and gas chromatography [16,17]. Figure 1-5 shows the two nozzle types frequently used. Typically, supersonic jet expansion is used for physical studies, to determine fluorescence spectral lifetimes and kinetics. It is not, due to dilution, typically used in trace analysis, but its value in determining characteristics inherent in a molecule is obvious: this technique is free from all matrix effects

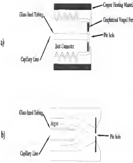

Figure 1.5 Simplified supersonic jet nozzles a) simple expansion nozzle, b) sheath flow nozzle. (Adapted from Reference 16)

However, sample types are limited to those which can be vaporized so that deposition of sample on the nozzle is avoided

Matrix Isolation

First described by Pimentel and co-workers in 1956, matrix isolation is a technique in which a gaseous sample is co-deposited with a gaseous matrix onto a cold stage and frozen In this way, the molecules are held in place so that a smaller number of sites may be excited thus, inhomogeneous broadening is reduced In this technique, only the emission spectra have narrowed bands [18] The matrix used can be any gas, but should be one which is optically transparent in the wavelength region of interest and which does not interact with the analyte. Frequently the matrix is nitrogen or argon The sample can be of any type, as long as it can be vaporized for deposition

Uses for the technique have been to capture short-lived species for study, to capture a reactive intermediate for further reaction in the observation area, and to create similar microenvironments for the analyte molecules, taking advantage of the decreased inhomogeneous broadening [1] The resulting spectra have narrower and resolved peaks The molecules do not fit in only one orientation in these matrices, however, and multiple sites still exist, creating significant inhomogeneous broadening In order to be used for qualitative luminescence information, a narrow linewidth source is necessary to minimize the sites activated The use of such a source to select a specific transition, or zero phonon line, is called "site selection spectroscopy" or "fluorescence line narrowing" [18 19]

Shpol'skii Spectroscopy

Freezing polycyclic aromatic hydrocarbons in an *n*-alkane matrix results in "quasi-line" spectra. This effect, first noted by E.V. Shpol'skii in 1960 [20], is due to a dramatic decrease in inhomogeneous broadening; if the chain length of the *n*-alkane matches the skeleton of the PAH, the "lock-and-key" fit of the analyte into the matrix limits the number of sites. Figure 1.6 demonstrates solvent analyte chain matching. In this technique, both the absorption and the emission spectra bands are narrowed [18]. Although the sites are limited, the crystal is not homogeneous, and inhomogeneous broadening is still significant. One factor controlling the homogeneity of the matrix crystalline structure is the rate of cooling, an effect demonstrated in Figure 1.7 [21]. Because this technique is based on the analyte fitting into the lattice of the *n*-alkane crystal, it is limited to those compounds which can fit into the lattice easily, that is to say, polycyclic aromatic hydrocarbons (PAH). For most applications, however, there is the advantage that the sample can be of any phase.

There are some drawbacks to this technique, however; the first is that each analyte has a different optimal solvent [22], and the solvent choice can cause a shift in the energies of the observed transitions, shown in Figure 1.8. It is also more likely that photodegradation of the analyte will occur in a matrix of its optimal solvent. The photodegradation has been attributed to a resonance effect. The excitation energy causes the matrix lattice to vibrate more strongly. If the lattice frequency is resonant with a vibrational frequency of the analyte, significant energy transfer may occur which can lead to degradation of the analyte [18,22]. Another limitation to the

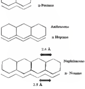

Figure 1.6 Relationship of solvent shape and dimensions to molecule dimensions Length and geometry are both a consideration Shown here are some molecules and their optimal solvents (Adapted from Reference 22)

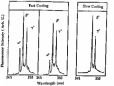

Figure 1.7 Effect of the rate of cooling on the sample homogeneity. As is seen, the number of sites is larger if the crystal is cooled too quickly. (Taken from Reference 21)

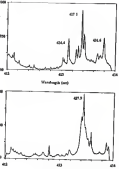

Figure 1.8 Solvent effect on the observed fluorescence emission spectrum of 7-methoxybenzo[a]pyrene. a) the top spectrum is 5 ppb in n-octane; b) the bottom spectrum is 500 pptr in n-decane. Note that the observed transitions are not at the same wavelengths, and that the intensity is greatly affected. (Taken from Reference 19)

technique is that it does not change the fact that isomers of a compound do not necessarily have the same quantum efficiencies; sensitivities may vary widely [23,24].

Site Selection Spectroscopy

Site selection spectroscopy is a technique which can be used with any of the low temperature techniques in order to diminish the effects of inhomogeneous broadening. Since multiple excited states can be populated in all of these techniques and since different sites have different zero phonon line positions, several absorption lines are possible. Site selection is an attempt to eliminate emission spectral contributions from interferents [25]. If an excitation source is chosen which has a narrower linewidth than the natural linewidth of the transition, then only the transitions corresponding to the energy supplied will be seen in the emission spectrum as very narrow lines [18]. This effect is seen in Figure 1.9.

In matrix isolation, site selection is nearly essential in that there are many sites in the matrix. While site selection allows any matrix to be suitable, a characteristic useful in that the spectral solvent desired is often a poor chemical solvent, the technique is not without its disadvantages [18]. The excitation wavelength must be determined through trial and error, it is likely in any given matrix that, not only will the zero phonon line of the analyte be excited, but also the phonon wings of interferents.

Previous Work

PAH compounds are of great interest due to their demonstrated carcinogenicity and mutagenicity [26]. They are created in the incomplete combustion of organic

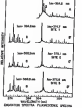

Figure 1.9 Site selection spectra of a 11 methylbenz[a]anthracene in n-octane. Three sites are present if non-selective excitation is used. The effect on the observed fluorescence spectra is seen when the three sites are selectively excited. The spectra on the left are excitation spectra, those on the right are of fluorescence emission. The fluorescence linewidths are noticeably narrower, and the spectra are far less congested (Taken from Reference 25)

matter and are found in great abundance in fossil fuels, and in exhaust from cars and diesel trucks. Because most PAHs are anthropogenic in origin, regulation of the pollution of the environment by petroleum companies and factories requires techniques which are able to identify and quantify the compounds. This is the application to which Shpol'skii spectroscopy is best suited, and an atlas of PAH spectra has been compiled [27]. Petroleum, soil, water, air particulate, and food samples have all been analyzed for PAHs using Shpol'skii spectroscopy [28,11,29]. Up until now, only fractionation has been used for the Shpol'skii detection of LC eluent [30,31], and no continuous sampling GC detector has provided viable results.

Jones and Winefordner [29] designed a self-cleaning Shpol'skii apparatus, which improved on the other systems available at the time in that it could be continuously sampling. All of those detectors required disassembly and warm-up time to change samples [31,32]. Clos created an interface so that continuous GC sampling was possible [33]. This system, however, had its drawbacks. The hexane used was part of a hexane-helium mixture and the ratio of matrix to solute was too low for isolation of the molecules. Additionally, the temperature and pressure of the system were too high for clearly resolved spectra.

Focus of This Work

This work describes a low pressure hexane reservoir which supplies a flow of hexane gas, and a dual transfer line so that the matrix ratio is optimized. In this way, the GC separation is unaffected by changing the flow of matrix gas. It is an improvement on the earlier work in that the high background signal has been eliminated, and the reproducibility of the belt speed is ensured.

A study was performed determining the optimal matrix to solute ratios using argon for matrix isolation studies, and performance of the matrix reservoir is evaluated.

Table 1. Comparison of Low Temperature Techniques

Criteria	Supersonic Jet Expansion	Matrix Isolation	Shpol'skii Spectroscopy
Sample Constraints	Must be vaporizable	Must be vaporizable	Must be soluble in Solvent, Non polar compounds
Instrumentation Required	Vacuum System (LASER)	Vacuum System Cryostat (LASER)	Vacuum System Cryostat White Light Source (LASER)
Predominant Broadening Mechanisms	Homogeneous	Inhomogeneous due to multiple sites	Inhomogeneous due to multiple sites
Matrix	None required Solvent effects are minimized Solvent shift of observed spectral lines can be eliminated and field splitting of lines due to solvent is eliminated[a]	Any gas optically transparent in the region of spectral interest Matrix causes shift in transition energy, and allows multiple sites Crystal field splitting likely, but not detectable compared to extreme inhomogeneity of the crystal	n-alkane, preferably of chain length which matches long axis of analyte Matrix causes shift in transition energy, allows multiple sites and crystal field splitting
Linewidth (FWHM)	0.01-1 cm^{-1} Limited by Excitation Source and Natural Linewidth	10-200 cm^{-1} [b] Varies With Matrix and Excitation Source	1-10 cm^{-1} [c]
Sample Recovery	Removed by Vacuum	Nondestructive	Possible photodegradation, Otherwise non destructive

[a] Reference 25
[b] Reference 31
[c] Reference 34

CHAPTER 2
LOW PRESSURE OUTLET GAS CHROMATOGRAPHY

First predicted by Giddings in 1962 [35], capillary GC separation where the outlet is under vacuum has several distinguishing characteristics. The vacuum outlet causes the average column pressure to drop, the linear velocity to increase, and the effects are far ranging. First, the analysis time is decreased as the carrier gas diffusivity is increased [35,36]. Secondly, there is greater chromatographic efficiency if short columns are used [37,38,39]. Finally, greater resolution may be observed under certain conditions [40,39]. Although Giddings is regarded as the first to examine this technique [35], Ettre was the first to use the technique in the laboratory [41]. Leclercq and Cramers have written programs to obtain optimal conditions for the separation [42]. In this chapter, the parameters governing these effects, as well as those which apply to this analysis method will be addressed.

Introduction

In order to discuss chromatographic phenomena effectively, several parameters must be defined. Table 2 gives a description of the mathematical symbols used, and their physical significance; the mathematical formulae used for their calculation are described below. The average linear velocity of the mobile phase (also designated v or $\bar{u}$) is calculated from experimental data using Equation 2.1.

Table 2 Definitions of Chromatographic Parameters and Symbols Used in This Chapter

Chromatographic Parameter	Definition
t_R	The retention time of a component in a mixture. This is calculated by measuring distance of the center of the peak from the mark designating the injection of sample and by multiplying the distance by the chart speed of the recorder. This signifies the amount of time that the component is retained in the column. The higher the retention time, the larger the extent of interaction between the stationary phase of the column and the component. (s)
t_o	The retention time of unretained components. Usually this is taken as the amount of time required for methane to pass through the column, and is measured from the chromatogram as described above. This is a measure of the time that a component requires to flow through the column without interaction. (s)
t_r	The corrected retention time; this accounts for the fact that even unretained components of a mixture require time to pass through the column. This is a more accurate means of comparing interactions within the column. (s)
L	The length of the column. (cm)
u	The linear velocity of the carrier gas (mobile phase) through the column (cm/s)
k'	The capacity factor of a component on a given column and set of conditions. This is a ratio of the corrected retention time of a component (t_r) compared to the retention time of an unretained component (t_o) (Unitless)
N	The number of theoretical plates or "efficiency" of a column for a given set of conditions. The idea is that many separations occur within the column as the fractions separated pass through the column, they undergo yet more separation to be further isolated into smaller fractions. This value is on the order of several thousands, usually in capillary columns. The higher the value of N for a given column, the better the separation ability of the column. (Unitless)
H	The "Height Equivalent Theoretical Plate" of a given column for a given set of conditions. This is the theoretical length of column required to achieve separation of two similarly retained components. (cm)

Table 2--continued

Chromatographic Parameter	Definition
h	The reduced plate height. For capillary columns, the lower case "h" is used to denote that the value is corrected for the greatly reduced column diameter. (Unitless)
R	The resolution of two sequentially eluting components of a mixture for a given separation. (Unitless)
D_g	The diffusion coefficient for a substance in the gas phase. This factor describes the relative ability for a substance in the gas phase to move. This factor is given in the units cm^2/s, and is typically on the order of 10^{1}.
P_o	The pressure of gas at the end of the column, "outlet pressure". (Pa)
P_i	The pressure of gas at the head of the column, "inlet pressure". (Pa)
P	The ratio of inlet to outlet pressures. (Unitless)
A	Longitudinal broadening term of Golay Equation. This term accounts for the fact that the analyte does not pass straight through the column but spreads out in the column longitudinally. (cm^2/s)
B	Resistance to mass transfer in the gas phase. This term is a measure of the relative ease that an analyte may have in establishing equilibrium between different regions in the mobile phase. (s)
C	Resistance to mass transfer in the liquid phase. This term accounts for the relative ease of passage of the analyte through the liquid film phase to achieve equilibrium. (s)
D	Extracolumn broadening term. This term is a correction factor to account for experimental data. It allows for the broadening effects inherent in the injection and detection processes. (s^2/cm)
f_1	The Giddings-Golay pressure correction factor. This factor corrects the D_g which is defined for atmospheric conditions for any difference in P_o and P_i. This factor has a range of values such that $1 < f_1 < 9/8$. (Unitless)
f_2	The Martin James pressure correction factor. This also corrects for variation from atmospheric pressure. This factor has a range of values such that $1 > f_2 > 3/(2P)$. (Unitless)

$$\bar{u} = \frac{L}{t_0} \tag{2-1}$$

It can also be obtained using Poiseuille's equation if the inlet pressure of the column is known, and the viscosity of the carrier gas, in poise, at the given temperature is known, as shown in equation 2.2, where η is the viscosity of the gas. The viscosity of the carrier gas does not change significantly with temperature, as shown for helium, in equation 2.3, where the viscosity is in cgs units, and the temperature in K [41].

$$v = \frac{3P_i r^2}{32\eta L} \tag{2.2}$$

$$\eta = \frac{\sqrt{mkT}(a)}{(\pi\sigma^2)} \tag{2.3}$$

In this equation, a is a constant specific to the gas, k is the Boltzmann constant, m is the mass of the gas and σ is the molecular diameter of the gas. The significant aspect of the viscosity factor is that the average linear velocity will drop slightly as the temperature changes in a temperature program, which affects the separation parameters measured. This effect is small, however, because the volatility of the analytes are enhanced at the higher temperatures allowing them to be retained for shorter periods of time [38].

The capacity factor of the column for a given component is calculated using equation 2.4

$$k' = \frac{t_r - t_0}{t_0} \tag{2.4}$$

Chromatographic peaks are assumed to have a Gaussian distribution, and the width measured at half its maximum height (FWHM) can be derived for such a peak, as shown in Figure 2.1.

With this information, the efficiency of a column can then be calculated from equation 2.5,

$$N = \left(\frac{t_R}{FWHM}\right)^2 5.54 \tag{2.5}$$

the plate height (H) can be calculated using equation 2.6,

$$H = \frac{L}{N} \tag{2.6}$$

and the reduced plate height (h) is calculated from equation 2.7, and the column diameter, d_c

$$h = \frac{H}{d_c} \tag{2.7}$$

The diffusion coefficient in the gas phase, can be calculated using Stokes' law, equation 2.8 where ρ is the density of the gas [40].

$$D_g = \frac{6\eta}{5\rho} \tag{2.8}$$

The values calculated using density at atmospheric pressure must be corrected for vacuum outlet conditions, using equation 2.9 [36], where, p_a is atmospheric pressure. It is clear that decreasing the outlet pressure causes an increase in the observed D_g values. This makes perfect

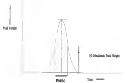

Figure 2.1 Determination of the FWHM value from a Gaussian Chromatogram peak

$$D_g=\frac{D_{gs}P_s}{P_o} \tag{2.9}$$

sense if one considers Boyle's law for gases, the decrease in ambient pressure allows gas to expand and reduce its density. Equation 2.8 shows that the diffusion coefficient should be increased under these conditions. The change in the diffusion coefficient has a significant effect, the kinetics of the interactions are faster under vacuum outlet conditions [36], hence analysis time will be decreased, and the optimal flow velocity will be changed without decreased separation efficiency.

Band Broadening in Chromatography

The plate height of an open tubular gas chromatography column is related to the velocity of the carrier gas in the Golay Equation, equation 2.10 [40]

$$H=\frac{A}{u}+(B+C)u+Du^2 \tag{2.10}$$

In this equation, A is the longitudinal diffusion term, B is the resistance to mass transfer in the gas phase, C the resistance to mass transfer in the liquid phase, and D is Gaspar's extracolumn broadening term [36]. For any set of operating conditions, there is an optimal velocity for the flow of the carrier gas at which the maximal efficiency is obtained in a reasonable analysis time. The optimal flow is determined by constructing a Golay curve of plate height versus the average linear flow velocity of the carrier gas. The optimal velocity is the velocity which corresponds to the lowest region of the curve. At low flow velocities, the A term dictates the shape of the curve. Near the optimal velocity, the B and C terms dominate, and at high velocities the D term is dominant. Vacuum outlet conditions affect the shape of the Golay curve, an effect that can be understood by examining the factors involved in determining the theoretical plate height. Figure 2.2 shows the Golay plot for four different outlet pressure conditions [37].

The value of A can be determined using equation 2.11 [37], Where P_i is the

$$A=3P_1\frac{D_{g1}}{P_i} \quad (2.11)$$

inlet pressure of the gas, and P_1 is atmospheric pressure. It has already been shown that D_g is increased at vacuum outlet conditions, thus the longitudinal diffusion (A) term is also increased.

The resistance to mass transfer in the gas phase is described by equation 2.12 [37], where r is the column radius.

$$B=\frac{(11k^2+6k+1)r^2P_i}{36P_1(k+1)^2D_{g,1}} \qquad (2.12)$$

This term is also dependent on the D_g term, and is decreased under vacuum outlet conditions. The resistance to mass transfer in the liquid phase is described by equation 2.14, where d_f is the thickness of the stationary phase film in an OTGC column [36]. The terms most significant in comparing the B and C terms involve the

$$C=\frac{2kd_f^2}{3(1+k)^2D_l} \qquad (2.13)$$

D_g, D_l, r, and d_f^2. In this work, P_i was 900 torr, and P_o was measured as (10^{-6}) torr, but was probably nearer to 100 mTorr locally [37]. For a temperature of 280 C, D_g has a calculated value of $6(10^{-2})$ cm^2/s. A typical values for D_l are 10^{-5} cm^2/s. In the

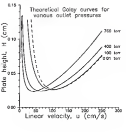

Figure 2.2 Golay curves on short columns at four different outlet pressures. Note that the difference between the 100 torr and 0.1 torr curve is minimal. This suggests that pressures below this value will exhibit no further improvement in analysis time. This data is for a 4 m column. (Taken from Reference 37)

OTGC column used in this work, the stationary phase film thickness was 2.5(10^{-5}) cm, and the radius was 3.2(10^{-2}) cm. For most values of k, the calculated value of B is on the order of 10^2 larger than C. Hence, in an OTGC column, the contribution of the C term can be considered insignificant, and the equation is simplified to

$$H=\frac{A}{u}+Bu+Du^2 \tag{2.14}$$

The Giddings Golay equation originally did not take into account outlet pressure effects. Data plots did not show a smooth linear region past the optimal velocity; rather, there was a curve upward. The D term due to extracolumn broadening is calculated as shown in equation 2.15, using σ^2 to describe the temporal band width from extracolumn sources, (extracolumn variance) in s^2 [36]. The total

$$D=\frac{\sigma^2}{L(k'+1)^2} \tag{2.15}$$

observed variance (σ_t^2) of peak broadening is described as the sum of extracolumn variance (σ_{ec}^2) and column variance (σ_c^2), shown in equation 2.16 [36].

$$\sigma_t^2=\sigma_c^2+\sigma_{ec}^2 \tag{2.16}$$

The Golay equation accounts for broadening on column, but the extracolumn variance can be seen as the sum of variances of two independent sources: the injection process (σ_i^2) and the detector effects (σ_d^2). Injection processes include broadening sources such as injector dead volume, sample loading, and syringe technique. Detector contributions to broadening include the detector time constant, and its dead volume. The extra column variance contributes significantly to the observed plate height, especially if higher optimum flow velocities are employed, as the D term has a squared dependence on the velocity It is important to note that the efficiency of the column is inversely proportional to the observed plate height. Therefore, low values of H are desirable

Analysis Time

A Golay curve for data taken under vacuum outlet conditions shows a shift of the optimum linear velocity to higher values This is due to the increased diffusivity of the gas under these conditions Because of the enhanced volatility, discussed earlier, the retention times of compounds are reduced, making it possible to perform rapid separations with no loss of efficiency [43] The optimal linear flow velocity for vacuum conditions is described by equation 2 17 where the subscript one means the value at atmospheric pressure [40]

$$v_{opt,vac} = \sqrt{\frac{P_1 3(1+k)^2 D_{g,1}}{2N(11k^2+6k+1)\eta}} \qquad (2.17)$$

If one considers that N is L/H, equation 18 can be rewritten as shown in equation 2 21

$$v_{opt,vac} = \sqrt{\frac{HP_1 3(1+k)^2 D_{g,1}}{2L(11k^2+6k+1)\eta}} \qquad (2\ 18)$$

This shows that the optimal velocity is closely related to the length of the column For comparison purposes, equation 2 19 gives the optimal velocity under atmospheric pressure outlet conditions.

Here the length dependence exists but is not as obvious, or as pronounced in

$$v_{opt,atm} = \frac{6D_{g,1}(P^2-1)}{r(P^3-1)} \sqrt{\frac{3(1+k')^2}{11k'^2+6k'+1}} \tag{2.19}$$

its effect. The pressure in a column is dependent on column length, as shown by equation 2.20 where the distance from the inlet, x, is defined by the following relationship:

$$P_x = \sqrt{\frac{(P_0^2 - P_i^2)x}{L} + P_i^2} \tag{2.20}$$

A gain factor can be calculated, taking the ratio of equations 2.18 and 2.19 the average linear velocities for vacuum versus atmospheric outlet conditions [40]:

$$G_v = \frac{v_{vac}}{v_{atm}} = \frac{r(P^3-1)}{(P^2-1)} \sqrt{\frac{P_1 H}{72 L \eta D_{g,1}}} \tag{2.21}$$

In this equation, P_1 and $D_{g,1}$ are defined for the atmospheric pressure conditions. It can be seen that shorter columns will allow higher linear velocity values than long columns. Additionally, wider bore columns should also allow faster analysis. Figure 2.3 demonstrates the effect of column length on the sensitivity of the separation to outlet pressure conditions.

Retention times are closely related to the diameter of the column being used, d_c. Equation 2.22 allows the determination of the optimal retention times for an analysis in an OTGC column

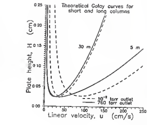

Figure 2.3 Golay curve for 2 lengths of column at two different outlet pressures. It is clearly seen that the long column experiences far less vacuum effect than a short column. Not that the optimum linear velocity is shifted to a higher value in both the long and short columns. (Taken from Reference 37)

$$t_R = \frac{(11k'^2+6k'+1)f_1 P_o d_c^2 N}{48(k'+1) f_2 D_{g,1}} \qquad (2.22)$$

This relationship is given for OTGC under vacuum outlet conditions by

$$t_{R,vac} = \frac{3(11k'^2+6k'+1)d_c}{16(k'+1)} \sqrt{\frac{2\eta N^3}{P_1 D_{g,1}}} \qquad (2.23)$$

equation 2 26[43].

Again, a gain factor can be calculated for retention time of systems under different outlet pressures For two OTGC columns under the same experimental conditions, having the same length and column diameters, this can be expressed using equation 2 24 [43]

$$G_L = \frac{t_{R,atm}}{t_{R,vac}} = \frac{d_c P_o}{8 f_{2,1} \sqrt{2\eta P_1 D_{g,1} N_{vac}}} \qquad (2.24)$$

Thus, the fastest separations occur with vacuum outlet conditions It is also seen that wide bore columns should be faster than narrow columns. This is easily understood considering that the conductance of flow is decreased as the diameter of the tube is decreased [44] Leclercq and Cramers found that vacuum outlet faster as long as the diameter of the column being used under vacuum is less than or equal to that being used at atmosphere Additionally, using high efficiency columns may not allow fast separations especially if the diameter of the column is very narrow [43]

The resolution of two components, here designated 1 and 2, which elute sequentially, can be calculated using the general resolution equation, equation 2 25, where α is k_2/k_1 [45]

$$R_s = \frac{\sqrt{N}}{4}[\frac{\alpha - 1}{\alpha}][\frac{k_2}{1+k_2}] = \frac{L}{H}(selectivity\ term)(capacity\ term) \quad (2.25)$$

Because the resolution is dependent on the square root of the efficiency, those columns which can be operated at higher efficiencies, such as short or wide bore columns, should have enhanced resolution. The efficiency gain of such columns is often large enough to offset the column length term. Under these experimental conditions, no such gain would be anticipated.

Effects of Vacuum Outlet Conditions on this Work

The experimental conditions and calculated values from this work are given below. The temperature of the transfer line was 280 C, the highest temperature in the temperature program. Values of k' ranged from 5-35, the column length was 25 m, and the value of D_g was 5.6(10^{-1}) cm^2/s. It is not expected that significant reduction in analysis time should be observed. The system has a no measurable effect on the observed dead time for the first-eluting compounds, it would be expected to be increased due to the added length of transfer line and fittings added to the column. It is obvious then, that the flow velocity was increased, most likely near the vacuum outlet. The later eluting compounds were delayed slightly, however. This may be due to the increased viscosity at higher temperature, and perhaps at this time, the true dead time could be detected. Another probable explanation for the observed delay of the heavier compounds is that there was uneven temperature control over the transfer line, causing cold spots and incomplete volatilization and band broadening.

The delay was about 1.5 min for the later eluting compounds, compared to their retention times for atmospheric FID detection. It should then be expected that the bands were broadened according to the Gaspar extracolumn broadening term. The column length was chosen to allow high loading capacity for the detector. While short columns are advantageous with regards to analysis time, their loading is low

CHAPTER 3
EXPERIMENTAL PROTOCOL AND INSTRUMENTATION

Spectroscopy

The radiation source shown in Figure 3.1, was a 300 W ILC Technology Cermax Model LX-300 xenon arc lamp source (Sunnyvale,CA), the entire output of which was chopped using an Ithaco, Inc. Model 382A chopper (Ithaca, NY). In this way, the sample was illuminated while the detector was blocked and source blocked while the detector was illuminated, so that scatter from the source and chamber could be eliminated. An adjustable aperture was used to shape the source spot to about 50 mm on the belt, and a 6 in focal length quartz lens was used to direct the source light onto the sample. A quartz water filter was used to decrease the heating effects of the source on the sample. The phosphorescence was then directed by a 6 in focal length quartz lens onto the focal plane of an Instruments SA, Inc. (Metuchen, NJ) Model UFS-200 flat field spectrograph. The spectrograph, in combination with the Princeton Instruments, Inc. (Princeton, NJ) Model IRY-700 photodiode array covered the spectral range of 200-800 nm, and the spectral interval per pixel was 1.4 nm. The data were collected by a Princeton Instruments, Inc. Model ST-120 OSMA Detector Controller, and a Club America (Austin, Texas) 286 personal computer with a math co-processor.

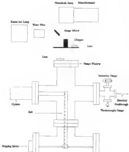

Figure 3.1 Vacuum chamber and optical configuration

Vacuum Chamber

The chamber was comprised of a Vac-U-Flat five-way cross, and a Vac-U-Flat three-way cross, each with 6 in flanges, a Vac-U-Flat three-way cross with 2.75 in flanges, a 6 in quartz viewing window, and two direct-drive rotary feedthroughs, all commercially available through Huntington Mechanical Laboratories (Mountain View, CA). The vacuum system consisted of a Model DUO-30A Trivac dual stage rotary pump, with 2 in tubing, a molecular sieve foreline trap, and a Model TMP-1000 turbomolecular pump, all obtained from Leybold-Heraus (Export, PA). Vacuum gauges, a Model 801 Thermocouple gauge, and a Model 572 Ionization Gauge were obtained from Varian Vacuum products (Lexington, MA). An electrical feedthrough on a 2.75 in conflat flange was obtained from MDC Vacuum Products Corporation (Hayward, CA). An APD Cryogenics, Inc. (Allentown, PA) displex Model CS-202 closed cycle helium refrigerator was used to maintain cryogenic temperatures. The vacuum system is shown in Figures 3.1 and 3.2.

The sample belt was custom designed by Belt Technologies, Inc. (Agawam,MA). This stainless steel belt was perforated at one side, and was driven by a ball-toothed spool, to prevent slippage and to ensure smooth, reproducible motion. It was 22.9 in long, 0.625 in wide, and has tooth spacings of 0.332 in. The belt passed over an oxygen free high-conductivity copper spool which bolted onto the cold stage of the closed cycle refrigerator. The spool measured 3/4 in diameter, and 7/8 in wide, and was created by our machine shop.

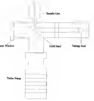

Figure 3.2 Side view of vacuum chamber

Chromatography

The chromatograph was a Perkin-Elmer Model 8500 Gas Chromatograph (Norwalk, CT) with a 30 m x 0.32 mm DB-5 capillary column. The high purity carrier gases were obtained from Alphagaz (LaPorte, TX).

The separation was carried out using a temperature program which started at 180 °C for 2 minutes isothermally, and the increased to 280 °C at a ramp rate of 3 °C/min. The final temperature was held for 5 minutes. The injector and detector were held at 290 °C. The total run time was 35.33 min. The injection was split 1000:1 at 0.4 min into the run, to purge excess solvent vapors from the injector.

Evolution of the Transfer Line Design

Phase One

The GC/Vacuum interface shown in Figure 3.3 was based on a design by Brown and Wilkins [46], and was the transfer line used by Clos [33]. The fitting had three essential components. The bottom piece, attached to a vacuum flange, was composed of a cylinder with coarse threading in its internal diameter. The central piece was a knurled cylinder with coarse threading on its exterior and fine threading on its interior. The top piece was a knurled cylinder with fine threading on its exterior. Ceramic tubing with a diameter of 1/4 in passed through the center of the three pieces. After passing through the first two pieces, the tubing passed through the center of five teflon compression rings. The tubing then passed through the center of the bottom piece, extending about one inch past the flange. The central piece was tightened, by hand, as far as it would go, to seal the compression rings around the

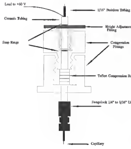

Figure 3.3 Interface design for first portion of work

ceramic tubing, isolating the top of the interface from the vacuum. The fine threading on the top piece allowed for height adjustment of the ceramic tubing. The flange had an o-ring groove and was sealed to the vacuum chamber with a viton o-ring.

The transfer line was a 1/16 in stainless tubing with a positive terminal lead soldered to it, about 1 in from the end of the tube on the vacuum side. The other end of the tube, located as close to the GC oven outlet as possible, had a ground lead clamped to it using a copper collar. The vacuum seal of the stainless tubing was made at a swagelock union which joined the stainless steel tube to the column, with a 1/16 in straight polyimide ferrule. From the GC side of the interface, the stainless tubing passed through the length of the ceramic tubing, extending 1 in past the end of the ceramic tubing on the vacuum side. The entire length of the tubing which was inside the ceramic tubing was wrapped in thermal insulating cloth. The length of the tubing which extended from the interface to the GC was in a braided ceramic sleeve to prevent heat loss. The stainless tubing passed through a drilled out swagelock 1/4 in to 1/16 in reducing ferrule, and the ceramic tubing was isolated from the vacuum with a 1/4 in graphite ferrule. The heating of the transfer line was accomplished using an SPC Technology universal step-down transformer distributed by Newark Electronics (Jacksonville, FL), which delivered 1 A of current, and a Variac which was operated at about 58% to maintain a temperature of 280 °C.

The sample was introduced to the chamber through the GC column which passed through the swagelock union joining the transfer line to the column, and was sealed to vacuum by a 1/16 in, 0.5 mm i.d. vespel ferrule. Problems with the interface design included that the transfer line was unheated for about 1 in, and that the electrical contact was very difficult to feed through the ceramic tubing without breaking the tubing or breaking the contact.

In the work by Clos [33], there was a significant background signal and the base pressure was 10^{-5} torr, without flow. Two factors contributed to this background, the vacuum pump had insufficient throughput to accommodate the added flow of the GC, and that from the molecular beam valve, used to deliver a small amount of hexane matrix. To minimize part of this problem, the turbomolecular vacuum pump used in this work had a significantly higher throughput (200 $\mathrm{l\,s^{-1}}$) than that used by Clos (75 $\mathrm{l\,s^{-1}}$) [33]. It was discovered at the start of this work , that the integrity of the vacuum seal created by the molecular beam valve was non-reproducible, and so the molecular beam valve was removed from the system. The result of these changes was that the base pressure of the system, with minimal flow was 10^{-6} torr. Some flow is required to minimize volatilization of the stationary phase of the GC column.

The first experiment performed involved matrix isolation in which the matrix, argon, was added to the mobile phase of the GC. The carrier gas was a 3% argon in helium mixture. The results of this initial experiment signified that the matrix ratio was not high enough to isolate the analyte sufficiently. It was desired that this ratio be controlled easily and that adjustment be possible.

Phase Two.

A dual capillary transfer line capable of greater control over matrix gas flow was the next step. In this way, the matrix could be added independent of the carrier gas, and any gas could be used, not just those in which the sample is soluble. Because two capillaries could not pass through a 1/16 in tubing easily, the interface was redesigned to accommodate a 1/8 in stainless tubing. This necessitated the replacement of the ceramic tubing as its inner diameter was not large enough to pass the 1/8 in tube. Criteria for the interface lining tubing were that the tubing be neither thermally nor electrically conductive. High temperature teflon tubing was used since it met these requirements. In order to ensure that the teflon tubing remained in place, two ferrules were seated on the teflon tube; one on top of the interface, the other placed on the opposite side of the top piece, as shown in Figure 3.4.

The electrical connections for the transfer line were as follows: the ground from a transformer was attached to a collar which fit around the swagelock union at the GC end of the transfer line. The other transformer lead was fed to an electrical feedthrough vacuum flange. A terminal loop was soldered to the tip of the stainless tubing, and a lead was bolted to the terminal loop and attached to the vacuum side of the electrical feedthrough via a Molex 93 terminal clip. The stainless steel tubing housed two capillaries, the GC column and a deactivated silica column through which the matrix passed. The capillaries were held in place by a Swagelock 1/8 in to 1/16 in reducing union with a two-hole ferrule. The stainless tubing was open on the end in the vacuum chamber, but was sealed from the atmosphere at the GC with a

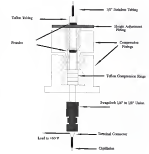

Figure 3.4 Dual capillary interface design

graphite ferrule. The entire length of the transfer line was surrounded by braided ceramic insulating sleeve.

The dual capillary worked satisfactorily, but voltage spikes in the power line caused super heating which melted both the electrical feedthrough teflon insulation and the teflon tubing. This design clearly needed improvement. The first change was to upgrade the electrical feedthrough to a high current application. In this way, the power surges would not cause meltdown, but a new insulator tubing was needed.

Phase Three

The final successful design of the transfer line was the simplest. The only real requirement of the interface was that it allow a resistively heated stainless tube to pass through it, and that the two capillaries also be accommodated. In order to achieve this, vacuum seals were needed from the insulated flange to the chamber, from the stainless tube to the interface, and from the stainless tubing to the capillary. Figure 3.5 shows the design of this interface. It consisted of a flange, which sealed to the vacuum chamber with a viton o-ring, and which had a 3/8 in swagelock bulkhead union mounted in its center. The insulated tubing was a 3/8 in ceramic tubing from Omega Engineering (Stamford, CT). The tubing had an internal diameter large enough to pass the 1/8 in stainless tubing with a significant amount of clearance. The ceramic tubing was sealed from the atmosphere with a 3/8 in graphite ferrule. The stainless steel tubing sealed to vacuum at the 1/8 in to 1/16 in reducing union with a 1/8 in polyimide ferrule. The capillaries fed through the 1/8 in tubing, and were guided into a fixed position by a 1/16 in-0.5 mm two-hole ferrule. Electrical

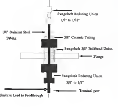

Figure 3.5 Final design of interface using bulkhead union. The stainless steel tubing extends one meter from the interface to the GC. It is not shown to scale.

connections were the same as in the previous design. Again, the stainless steel passed through a braided ceramic sleeve.

Matrix Isolation

The capillary carrying the matrix argon was fed through the injector of column 2 of the GC, and out the detector 2 port. In this way, the effective flow ratio through the two columns could be kept proportional through the temperature program. A length of deactivated silica was installed to serve as column 2, and which passed through the detector port, and fed through the 1/16 in to 1/8 in reducing union and through the 1/16 in-0.5 mm 2-hole reducing ferrule. Both columns passed through the length of the 1/8 in stainless steel tubing. The matrix ratio was varied by varying the flow rate of argon through column 2. The flow rate of argon was determined using a soap bubble flowmeter, measuring the flow at the end of the transfer line. The argon was regulated at the tank, and two needle valves were placed in line before the column. The micrometer calibration on the needle valve allowed crude, but reproducible adjustment of flow. The valves were calibrated to determine the necessary parameters for a desired flow, that is, the tank pressure, and the position of each needle valve. In this way, the very low flow rate required for this study could be controlled.

The pressure of the system, with the transfer line in place and with flow from the GC, was approximately 10^{-5} torr, and the cold head temperature was 17 K.

Shpol'skii Matrices

For the Shpol'skii matrix studies, the tank of argon and GC flow controller were replaced by a stainless steel hexane reservoir. Figure 3.6 shows the hexane

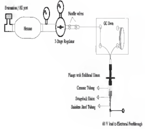

Figure 3.6 Hexane Reservoir design for dual capillary matrix isolation

reservoir supply. The reservoir was a 300 mL stainless steel sample cylinder from Jax Valve (Jacksonville, FL). Each end of the cylinder had 1/4 in Female Normal Pipe Thread (FNPT) fittings. A brass valve was attached to one end of the cylinder to allow the cylinder to be evacuated, and filled with hexane. The other end of the cylinder also had a 1/4 in brass valve to allow the cylinder to be isolated during the evacuation and filling procedure. This end also had a low pressure gauge from Matheson Gas Products (Secaucus, NJ) so that the pressure in the cylinder could be monitored, and a single stage low pressure gas regulator. The output from the gas regulator was fitted to a 0.32 mm o.d. deactivated silica capillary, which was fed through the injection septum of the second column of the GC into the oven. The capillary continued out the detector port for the second column and fed through the transfer line as had the argon capillary. Regulation of the hexane supply was through heating the cylinder in a water bath, according to the relationship shown in Figure 3.7, and described by the following equation, where the values for hexane are A = 7627.2, and B=7.717, temperature is in K, and pressure is in torr.

$$\log P_{saturation} = -0.2185\frac{A}{T} + B$$

The flow was then regulated through the low pressure regulator, and the needle valves as before.

Reagents

Reagents were used as received, without further purification. Stock solutions in *n*-hexane were made of each at the concentration of about 100 *ppm*, and standard

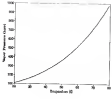

Figure 3.7 Saturation pressure curve for hexane

mixtures were prepared for the range from 0 5 to 100 ppm of each component. Table 3 lists the reagents and their sources

Procedure

To start the system, the roughing pump reduced the pressure to 100 mtorr The turbo pump then reached a pressure of 10^{4} torr At this time, the belt motor and cryostat were switched on The belt was running while the system was cooled so that the belt would not freeze to the cold head When the cryostat reached 13 K, the flow on the chromatograph was increased by increasing the column head pressure to its operating pressure of 19 psi

Table 3. Reagents

Reagent	Purity (%)	Source
n-Hexane	UV-grade	Burdick & Jackson Muskegon,MI
Fluorene	98	Eastman Rochester, NY
Triphenylene	96	Aldrich Milwaukee, WI
1,2 Benzofluorene	98	Aldrich Milwaukee WI
2,3-Benzofluorene	98	Aldrich Milwaukee WI
Phenanthrene	98	Eastman Rochester, NY

The added flow from the GC caused the temperature to rise to the operating value of 17K The transfer line and oven were then allowed to heat to their operating temperatures. When the system was ready, the xenon arc lamp and chopper were started, and the diode array initialized. With flow, moving belt, and heated transfer line the operating temperature was about 19 K and the chamber pressure about $8(10^{-6})$ torr

The belt speed was the same as the chart recorder speed, so that the peak widths could be compared to that of the FID at room temperature;with the belt speed at 10 mm/min, spectra were collected every 10 s, and 10 scans were integrated for each spectrum

CHAPTER 4
RESULTS AND DISCUSSION

At the outset of this work, there were several problems to be addressed. While a self-cleaning, continuously sampling GC interface had been constructed, it had serious limitations: poor sensitivity and high background signal [33]. Due to the low volatility of hexane, the amount present in commercial gas mixtures was not sufficient to isolate the analyte molecules, resulting in poor Shpol'skii spectra. The background signal of the system, shown in Figure 4.1, was large and spanned most of the spectral region occupied by analyte luminescence. It was suspected that the vacuum system was inadequate for the flow of sample being introduced. In the system that existed, a molecular beam valve introduced flow of a hexane-helium mixture and the capillary column introduced the eluent from the GC. The self-cleaning mechanism of the detector depended on the vacuum being adequate for volatilization of the analyte as it moved off of the cold head after analysis. This feature was shown to be fully functional with discrete injection of sample, with no residual signal after sampling was complete [29]. The pressure of the chamber was elevated, and the volatilization (self-cleaning) efficiency was decreased.

A thorough examination of all of the components showed that the molecular beam valve did not seal to vacuum reproducibly. Thus, while the valve was in the closed position, a significant leak existed. Therefore, the molecular beam valve was

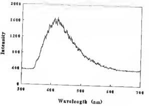

Figure 4.1 Background signal of LTMLS detector at the start of this work (Taken from Reference 33)

removed from the system, yielding a base pressure two orders of magnitude lower than that obtained in the earlier work [33]. Restoring the column flow raised the pressure one order of magnitude, as expected, and the background signal was still observed, although diminished to about one half of its previous value. It became clear that a higher throughput vacuum system was required; it was also necessary to reevaluate the method of matrix addition.

To reduce the operating pressure, several vacuum configurations were attempted, including the addition of a diffusion pump before the turbomolecular pump; none of these configurations was successful. When a 10 in turbomolecular pump became available, it was substituted for the 2.75 in turbomolecular pump, resulting in the disappearance of the previous background signal. This new turbomolecular pump had two advantages: first, it was roughed by a pump with about three times the pumping speed of that previously achieved, and second, the conductance of the larger turbo and vacuum hoses was about four times that previously used. The new background signal is shown in Figure 4.2; it is uncorrected for dark current, for comparison to the earlier data.

The first experiments were performed using the Flame Ionization Detector (FID) for the GC. The FID was primarily used to determine optimal separation conditions, and to determine the retention times for the test compounds on the column. Table 4 contains a comparison of the retention times for the standard solutions, using the FID versus that using the LTMLS. Sensitivity of the FID was

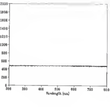

Figure 4.2 Background spectrum taken after renovating the vacuum system and removing the molecular beam valve

not consistent, due to an electronics failure so analytical sensitivity could not be determined accurately from the data.

Table 4 Retention Times of Test Compounds (in Minutes) under Atmospheric and Vacuum Outlet Conditions

Compound	FID	LTMLS
Fluorene	8.4	7.5
Phenanthrene	13.5	12.5
1,2-Benzofluorene	25.8	26.0
2,3-Benzofluorene	26.3	26.5
Triphenylene	33.0	35.0

In the first attempt at phosphorescence detection of matrix isolated species, the helium carrier gas was replaced by a 3% argon in helium mixture. It was hoped that by using argon in the carrier gas, not only would the system be simplified but also the pressure be decreased since no extracolumn gas flow was added. The results showed significant aggregation effects of the analyte molecules, peak heights were low and multiple broad bands were seen rather than a sharp central band. Fluorene was the only compound which gave peaks large enough to be detected, and then only at high concentrations. This experiment demonstrated the need for precise control over the amount of argon that could be added, that is, the ratio of argon to analyte deposited on the cold belt. The cost of multiple commercial gas mixtures would be prohibitive, and so it was desired that a means of adding a controlled amount of matrix gas be found. Figure 4.3 shows a matrix isolation phosphorescence spectrum of 67.5 ppm fluorene in 3% argon carrier gas. Here, the predominant feature is the delayed fluorescence peak on the left and the phosphorescence spectrum in the center. The

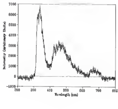

Figure 4.3 Phosphorescence matrix isolation spectrum of 67.5 ppm fluorene, background corrected, in 3% argon carrier gas. The sample mass was 0.34 μg. The primary feature of the spectrum is the delayed fluorescence peak on the left, and fine structure is absent.

feature on the right is not known, although it may be excimer fluorescence.

It was not immediately recognized that the aggregate peak was actually delayed fluorescence arising from a triplet triplet annihilation mechanism. Because phosphorescence is not a highly favored process, the signals obtained are generally weak. In the initial studies used to align optics and to identify the analyte signal, the standards used were of fairly high concentration. In this case, the use of high concentration standards was a particularly poor choice. Delayed fluorescence, column overload, and incomplete isolation of the analyte molecules were all results of this seemingly innocuous initial step. The phenomenon of the delayed fluorescence will be addressed at the end of this chapter, as it affected all phases of the data obtained.

A dual transfer line was next designed to allow pure argon to be added to the system, the argon could be added independently from the eluent of the chromatograph. In this way, the argon would not interfere with the separation, and by controlling the flow of the argon, an optimal ratio could be found of solute to solvent. The challenge lay in obtaining flow rates of about 0.1 mL/min, as this was the amount required to obtain a 1000:1 ratio of argon molecules to analyte molecules, a minimum ratio generally thought sufficient for effective isolation [47].

A low pressure regulator, in line with two needle valves, was used to regulate the argon flow rate from the argon tank to a capillary column. The flow rate was measured for several different settings of tank pressure, and individual needle valve settings. Figure 4.4 shows the data obtained from adjustment of the second valve

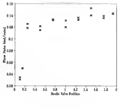

Figure 4.4 Flow rate calibration curve for needle valve control of gas tank. The regulated tank pressure was 6 psi The first needle valve was open to a set position

with a constant valve setting for the first valve. While the adjustment was crude, it was highly reproducible in terms of measured flow.

Matrix isolation studies were performed using a flow of 0.5 mL/min of argon in addition to the flow from the gas chromatograph. Figures 4.5 through 4.9 show the luminescence spectra taken when 5 μL of standard mixture solution was injected. The hexane eluted from 1-3 min in the run, and the first component eluted at about 8.5 min. After the first few samples, the spectra were only recorded after the hexane eluted to reduce the size of the files. The observed luminescence was most likely a combination of delayed fluorescence and phosphorescence spectra, the spectral resolution was poor due to the large number of sites excited simultaneously.

It was noted that the isomers, 1,2-benzofluorene and 2,3-benzofluorene showed no significant differences in their spectral shapes. This was probably a result of multiple sites being excited. It is known that the two isomers have significant overlap in their fluorescence spectra [48], and the spectrometer was low resolution in order to scan the wide range of wavelengths. It was also noted that, if the sample was allowed to deposit onto frozen hexane (the result of collecting all of the eluent in one spot), the signal was dramatically enhanced. A phosphorescence spectrum taken when the sample was deposited on hexane is shown in Figure 4.10. Therefore, even though the sample molecules were not completely isolated from one another, the immobilization in the lattice structure of the hexane was sufficient to achieve much higher spectral resolution. Another means of achieving the desired signal intensity would be to use laser excitation. The excitation wavelength from a tunable dye laser would allow

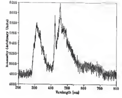

Figure 4.5 Matrix isolation luminescence spectrum for 67.5 ppm fluorene in argon. The sample mass was 0.34 μg, and the argon flow was 0.5 mL/min.

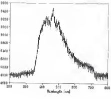

Figure 4.6 Matrix isolation luminescence spectrum for 81.5 ppm triphenylene in argon. The sample mass was 0.41 μg, and the argon flow was 0.5 mL/min

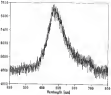

Figure 4.7 Matrix isolation luminescence spectrum for 131 ppm 1,2-benzofluorene in argon. The sample mass was 65 μg, and the argon flow was 0.5 mL/min

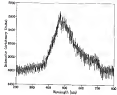

Figure 4.8 Matrix isolation luminescence spectrum for 114 ppm 2,3-benzofluorene in argon. The sample mass was 0.57 μg, and the argon flow was 0.5 mL/min

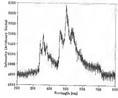

Figure 4.9 Matrix isolation luminescence spectrum for 65.5 ppm phenanthrene in argon. The sample mass was 0.33 µg and the argon flow was 0.5 mL/min

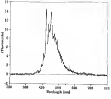

Figure 4.10 Phosphorescence spectrum for 67 5 ppm fluorene deposited onto hexane The sample mass was 0 34 μg, and the spectrum was corrected for background

detection of only selected phosphorescing compounds, and so it was decided to try another matrix suitable for multiple species detector Because the signals were low for such relatively high analyte concentrations, and because the spectral resolution of the matrix spectra was poor, a means of introducing hexane vapors was desired

Throughout the study, fluorene consistently demonstrated a strong signal The resolution of the spectra changed with the ratio of analyte to matrix and the type of matrix However, even if the amount of matrix was small and the ratio was less than 1000 1, fluorene could be detected. Due to its intense phosphorescence and sensitivity to the matrix to analyte ratio, fluorene was an excellent probe molecule for experimental conditions

A deactivated silica column, while desirable as a transfer column because of its lack of interaction, was abandoned after many attempts to achieve reproducible results The problem involved the poor seals made in the union connecting the column to the deactivated silica column. Many unions were tried, from different manufacturers and of different designs, with disappointing success rates It was therefore decided to eliminate the deactivated silica column and to pass the column directly through the transfer line, bypassing the union

A study was performed, using 5 μL of various concentrations of fluorene standard The matrix isolated phosphorescence spectra can be seen in Figure 4 11 Several interesting characteristics can be noted from these spectra First, the appearance of an ill defined secondary peak to the left of the primary peak was noted This peak was attributed to aggregation effects (incomplete isolation of the analyte

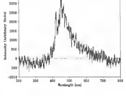

Figure 4.11 Matrix isolation phosphorescence spectra for fluorene in argon, corrected for background The argon flow was 0.5 mL/min and sample mass a) 0 006 μg .

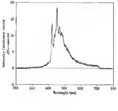

Figure 4.11--continued b) 0.02 μg.

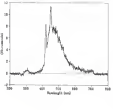

Figure 4.11—continued c) 0.07 μg.

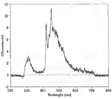

Figure 4.11--continued d) 0.10 μg.

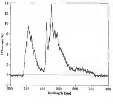

Figure 4.11--continued e) 0.34 μE.

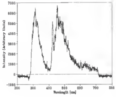

Figure 4.11--continued f) 0.41 μg

molecules), because it grew more prominent with increased analyte concentration (hence decreased matrix to analyte ratio). This same peak could be seen emerging as the chromatographic peak built, demonstrated in Figure 4.12. The leading edge of the chromatographic band has a relatively low analyte concentration, resulting in the appearance of the central fluorescence peak. As the chromatographic peak grew with time, the secondary peak emerged. This data clearly demonstrates that ratio of matrix to analyte was a very important factor in the peak shape. If an analyte is to be identified using this technique, it must be under the appropriate matrix conditions for best peak shape and resolution. The secondary peak here, too, can be attributed to delayed fluorescence because of its long lifetime and its spectral wavelength range. A means of confirming this assignment would be to perform a study in which the intensity of the excitation radiation is varied. If the mechanism observed had been a biphotonic process, a plot of the intensity of fluorescence versus the square of the phosphorescence intensity would be linear. Because of equipment failure, this experiment could not be performed [49].

The final phase of this work was to use a hexane reservoir to deliver hexane as the matrix. A chromatogram of the luminescence spectra in a Shpol skii matrix for a 70 ppm standard PAH mixture is shown in Figure 4.13. The major spectral features shown in Figure 4.13 are all attributed to phosphorescence, and the results for this phase were promising. The delayed fluorescence peak disappeared completely for phenanthrene and fluorene when hexane was added, demonstrating improved isolation capabilities of the hexane matrix. Additionally, fine structure began to appear in the

---

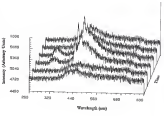

Figure 4.12 Matrix isolation phosphorescence and delayed fluorescence spectra of 20.25 ppm fluorene standard as chromatographic peak develops. The sample mass was 0.10 μg, and the time span 5.5-7.5 min, at 0.4 min intervals

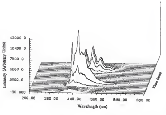

Figure 4.13 Shpol'skii luminescence spectra of 70 ppm standard mixture. Sample mass was 0.35 μg and the time span shown, at 0.5 minute intervals a) 3-16 min,

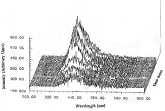

Figure 4.13--continued b) 16-29 min;

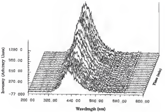

Figure 4.13--continued c) 29-40 min

spectra for phenanthrene. Figure 4.14 is a comparison of luminescence spectra of phenanthrene taken with a matrix of argon versus that of hexane. In hexane, only the phosphorescence peaks are present, but in argon, the delayed fluorescence peak appears. Again, the later eluting compounds were not clearly resolved, and had lower signal than is ordinarily obtained, suggesting that these compounds were not isolated effectively. However, it is clear that hexane was being delivered to the belt, and it was expected that modification of this reservoir would yield better results. At this point in the research, the vacuum pump bearings burned out necessitating the termination of the project.

Several features could be distinguished in the chromatographic data. Due to the poor intensity of phosphorescence signal of the later eluting compounds, their chromatographic peaks cannot be effectively analyzed. As would be expected for vacuum outlet conditions, the retention times for fluorene and phenanthrene were slightly decreased from their atmospheric outlet values; those for the later eluting compounds were delayed slightly. This was probably due to a cold spot in the transfer line, and suggested the need for more uniform heating of the transfer line. About 1 in of the column was exposed to the atmosphere between the GC outlet and the union which sealed the capillary inside the transfer line. A new transfer line, which allowed placement of the union to the vacuum inside the oven, was created but was never tested due to the failure of the turbomolecular pump.

Another aspect of this technique involves the decision of which luminescence wavelength should be monitored for chromatographic data. Figures 4.15-4.17 show

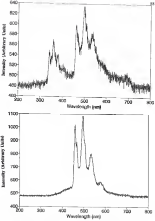

Figure 4 14 Luminescence spectra of 65 5 ppm phenanthrene standard in different matrices a) 0 33 μg sample in argon b) 0 13 μg sample in hexane

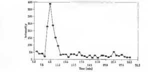

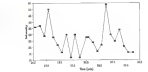

Figure 4.15 Chromatogram of five-component mixture, scanned at 340 nm The top spectrum is for the entire time range, the bottom spectrum is for the time after fluorene has eluted

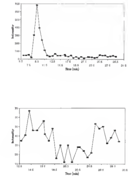

Figure 4 16 Chromatogram of five-component mixture, scanned at 360 nm The top spectrum is for the entire time range, the bottom spectrum is for the time after fluorene has eluted

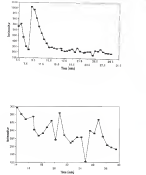

Figure 4 17 Chromatogram of five-component mixture, scanned at 500 nm the top spectrum is for the entire time range the bottom spectrum is for the time after fluorene has eluted the chromatographic data taken at different detection wavelengths Fluorene had peaks in all of the wavelength ranges, and its intensity was much greater than that for the other analytes under these experimental conditions Because each analyte has an optimal wavelength for analysis, no single wavelength detection would be suitable From the detector wavelengths evaluated, 340 nm appears to be the best for all of the substances.

In the chromatograms, it can be seen that the peak widths were very broad, an doubt due to column overloading For reference spectra taken of the individual standards multiple injections of standard were used, while the belt was held stationary, to attain a larger signal of sample. The sample volume injected for the five-component mixture was also high, at 5 μL A fairly slow ramp rate was used so that a more complex mixture would be separated, which was the goal of this work originally For the five-components studied here, it was far too conservative and led to broader peaks than would be preferred, at best quantitation would be difficult for data obtained under these conditions In order for this technique to have been used for quantitative analysis an internal standard may be used, and has proven successful for relative intensity comparison [50] An internal standard corrects for injection error and signal variations due to optical alignment or source fluctuations[3]

Because of the wide wavelength range (200-800 nm) observed in this study, the resolution was necessarily low (1 4 nm/pixel) The comparison literature was that for low temperature spectra, and most were obtained at much higher resolution than that employed in this work, subsequently, the delayed fluorescence was not immediately recognized Additionally, matrix isolation spectra of these compounds were not found in the literature Deviations in peak shape, intensity, and spectral position are expected in differing matrices, hence the conclusion that the matrix isolation was observed was incorrect and premature conclusions were drawn at this phase of the work

Finally, the appearance of delayed fluorescence must be discussed In the introduction chapter, a simple model of molecular excitation and deactivation was described There are other processes which can occur involving the deactivation of molecules in excited triplet states. they may form a dimer which is in an excited singlet state (an excimer) which then may fluoresce, they may collide transferring energy and quenching the phosphorescence, and they may be close enough to one another that they transfer energy to form a ground state molecule and an excited singlet state molecule (triplet-triplet annihilation) In general, excimer fluorescence is shifted to lower energies than normal fluorescence, the quenching process results in no observed luminescence, and triplet-triplet annihilation produces observed fluorescence identical to the normal fluorescence spectrum Another means of delayed fluorescence may be observed in the event of thermal excitation of the molecules but this event is highly unlikely at temperatures lower than 77K [49]

Figures 4 18 21 show the delayed fluorescence and phosphorescence spectra observed for some of these compounds. It can be seen that the secondary peak is nearly identical to that of the fluorescence of fluorene, phenanthrene, and triphenylene No recorded phosphorescence spectra were found for the benzofluorene

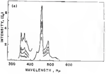

Figure 4.18 Delayed fluorescence spectrum for triphenylene in EPA at 77K shown at left, phosphorescence shown to the right (Taken from Reference 51)

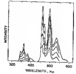

Figure 4.19 Delayed fluorescence spectrum for phenanthrene in EPA at 77K shown at left, phosphorescence shown to the right (Taken from Reference 52)

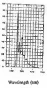

Figure 4.20 Fluorescence spectrum of 2,3-Benzofluorene (Taken from Reference 53)

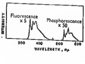

Figure 4.21 Delayed fluorescence spectrum for fluorene in EPA at 77K shown at left, phosphorescence shown to the right (Taken from Reference 54)

isomers, although the fluorescence spectrum for 2,3-benzofluorene was found to match the observed spectra.

CHAPTER 5
CONCLUSIONS AND FUTURE WORK

The focus of this work was to develop a phosphorescence detector capable of detecting PAH fractions from a GC as they eluted from the column. Such a system should be able to sample continuously, be self-cleaning, and be reproducible. It was also desired that the detector be versatile so that different spectroscopic conditions could be accommodated. The objectives were that the detector couple separation resolution with spectral resolution. Thus, varying experimental conditions and interfaces to find the most promising conditions and system was the means of approaching the problem. This work was a feasibility study, and was not meant to be quantitative, but was meant to explore the possibilities of new directions for instrumentation with the focus of finding a detector capable of analyzing complex environmental samples.

In the work done by Jones [29], the chamber was self-cleaning, but only discrete samples could be observed. The method required that several injections be made until the optimal position of the sample bead was achieved. With practice this was minimized, but reproducibility suffered, and time was wasted. In the work by Clos [33], placement of sample by the capillary reduced greatly the radius of the sample spot and prevented the belt from freezing to the cold head of the cryostat. However, with the reproducibility of capillary sample introduction came the disadvantage that sample loading was decreased about tenfold. Additionally, in the work by Clos [33], the belt was motorized expanding the utility of the detector to continuous sampling operation. However, the motion was sporadic, the belt slipped and did not move at an even pace. In addition, the system exhibited a high background signal.

In this work, most of the drawbacks of the previous systems [29,33] were addressed. Performing the sample belt and changing to a gear drive, made the belt motion smooth and reproducible. By increasing the throughput of the vacuum system and devising an alternate method of adding the matrix gas, the high background exhibited in previous work was removed.

The GC transfer line design used in the previous work was very awkward and fragile. To eliminate this problem, the bulkhead design was developed in this work and was found to be simpler and more sturdy. Its simplicity also allowed greater ease in positioning the capillaries. Although the interface used by Clos [33] had a feature allowing capillary positioning, it was ineffective. The bulkhead interface used in the present studies positioned the capillary close to the belt without touching it, and sample was deposited evenly and reproducibly.

The dual capillary transfer line created in this work, allowed deposition of the sample along with the matrix of choice. In this way, the separation was not affected by the addition of a matrix gas to the carrier gas. The use of two capillaries did not increase the pressure noticeably from that of a single capillary, allowing this method to be operated under lower pressure conditions than before [33].

The solvent reservoir developed in this work was very promising. Currently, the common means of adding liquids to vacuum is through the use of a Knudsen cell, a cell in which a sample is placed and heated; sample is allowed to flow through an orifice in the cell to the system. Alternately, a bulb of liquid is placed in line with the vacuum system so that the liquid is volatilized at the reduced pressure and drawn into the vacuum chamber. In both of these sample delivery methods, there is a finite sample volume, and no flow control. The solvent reservoir was capable of delivering the hexane, demonstrated by the enhanced resolution of the spectra taken with it. The solvent flow could be controlled, and it was easily refilled without breaking vacuum. Further study was needed to optimize its performance, as only two of the components received benefit of isolation. Phosphorescence signals were seen for the later eluting compounds, however, which did not occur in the absence of hexane.

The greatest difficulties encountered along the way involved the heating of the transfer line. This work modified the design previously used by Clos [33]. In retrospect, it is clear that a transfer line of silica lined stainless steel would have been more appropriate in that the electrical leads could be connected directly to the transfer line and because the heat transfer to the sample would be more efficient. The gap between the sample capillary and the walls of the transfer line were under vacuum, hence served a thermal insulation capacity. The measured temperature of the transfer line was not an accurate measure of the temperature to which the sample was subject.

Additionally, a slightly more elaborate electrical control was necessary for this system. Much time and effort was spent repairing and reworking the electrical system Voltage spikes that normally passed through the electrical lines wrought havoc on the observed temperature of the transfer line. Melted electrical components, scorched capillaries were common problems It was also not clear as to how uniform the heating was If there were cool spots in the transfer line the later eluting compounds would be retained far more than they should have been Because the chromatographic peaks for the later eluting compounds were broadened, it was assumed that such cold spots existed Additionally, there was no means of measuring the temperature inside the chamber It was suspected that the temperature inside the chamber was higher than that outside because of decreased collisional energy transfer

While the solvent reservoir was simple in design, elegant, and inexpensive, difficulties were encountered in its use, especially in the means of its heating A water bath was used to heat the solvent cylinder but the maximum achievable temperature with the water bath used (due to its enormous thermal transfer with the surroundings) was only 70 °C If the reservoir were maintained at a higher temperature, the flow rate of solvent vapor would greatly increase. Additionally, a larger cylinder would be useful. The cylinder used required refilling after about two hours of operation The refilling process was quite simple, however, because as the hexane was withdrawn by the vacuum, the refill hexane was drawn into the reservoir when the fill valve was opened

The data collected showed that the amount of matrix added had a large effect on the signal intensities and peak shapes These studies also underscored the importance of selecting the correct matrix for low temperature techniques The phosphorescence signal increased considerably with hexane compared to argon, which showed the utility of such an optimization In order to obtain good quantitative data, the ratio of solute to solvent must be fairly consistent to avoid peak height variations due solely to aggregation effects Due to the differing quantum efficiencies of different compounds, it may be useful to optimize this ratio for select test compounds.

For qualitative information, four parameters can be controlled the solvent type, the solute to solvent ratio, the excitation wavelength, and the excitation linewidth If the optimal solvent or solvent ratio is not used, it is imperative to use a narrow linewidth excitation source to reduce the number of sites excited This will have the disadvantage of selecting certain compounds, and omitting many others, however For many of the PAH compounds, however, it is likely that there will be a compromise excitation wavelength

Future Work

This work demonstrated the feasibility of a dual capillary transfer line, and of a solvent reservoir for a source of matrix For future work, it would be useful to redesign the chamber in order to decrease the length of the transfer line, decreasing the possibility of cold spots Additionally, the largest flange on the vacuum chamber was six inches The turbomolecular pump used had a ten inch flange, meaning that its conductance capabilities were not used to their greatest advantage. The new chamber would have a full ten inch flange, which would allow the base pressure of the system to be decreased, and should increase sensitivity

The solvent reservoir should be increased in capacity, and heating should be done in an insulated furnace which conformed to the shape of the cylinder. The cylinder was rated to a pressure of 1200 psi, and so it was unlikely that an explosion could occur. With these changes, the reservoir would be useful for a longer period of time, and higher temperature could be achieved, resulting in increased vapor flow.

To protect against voltage surges and to ensure reproducible heating, an electronic feedback circuit, similar to that used by Hall [37] should be used. Finally, it is clear that white light is not a viable source for such a detection method. Even the wavelength selection afforded by a monochromator would be sufficient to reduce the observed spectral linewidths and enhance spectral resolution.

From these studies, several conclusions can be drawn. First, if a Shpol'skii solvent is available for analytes being observed, its use as a matrix would be highly advantageous. Shpol'skii spectra taken in an appropriate solvent have higher intensity lines, decreased linewidths, and enhanced resolution than spectra taken in other matrices. Not all compounds have such an optimal solvent, but matrix isolation in argon still allowed enhancement of the phosphorescence signal. It was clear, however, that care should be taken to optimize the flow rate of the matrix to ensure adequate isolation of the analyte molecules. In addition, a narrow linewidth source is a necessity for matrix isolation spectroscopy if Shpol'skii solvents are not used, requiring that excitation wavelength selection studies must be performed.

Due to the minimal residence time of the sample on the cold head, it is not likely that scanning the excitation wavelength would be feasible, and the data files would be enormous for a chromatographic separation.

Finally, it would be useful to employ a high resolution spectrometer, such as an echelle polychromator with CCD (Charge Coupled Device) detection. The detection of complex samples required that a wide range of wavelengths be monitored. With a photodiode array, this required that a low resolution monochromator be used, and so the spectrograph may not be capable of differentiating fine structure. The use of a high resolution system, such as an echelle polychromator with CCD detection would give high resolution spectra over a broad wavelength range. Such a detection system would couple the advantages of the high throughput and resolution of the echelle system with the multi-dimensional array of the CCD. Such spectrographs have recently been used with success in ICP analysis [55,56], and seem ideally suited for this type of analysis.

REFERENCE LIST

1. Nakhimovsky, I., Lamotte, M., Joussot-dubien, J. "Handbook of Low Temperature Electronic Spectra of Polycyclic Aromatic Hydrocarbons," Elsevier New York (1989)

2. Ingle, Jr., J. D., Crouch, S. R. "Spectrochemical Analysis," Prentice Hall Englewood, NJ (1988)

3. Skoog, D. A. "Principles of Instrumental Analysis," Third Ed., Saunders College Publishing New York (1985)

4. Hurtubise R. J. "Phosphorimetry Theory, Instrumentation, and Applications," VCH Publishers, Inc. New York (1990)

5. Ramis Ramos, G. Garcia Alvarez-Coque, M. C., O'Reilley, A. M., Kashawneh, I. M., Winefordner, J. D. *Anal. Chem.*, **60**, 416 (1988)

6. Perry, L. M., Campiglia, A. D., Winefordner, J. D. *Anal. Chem.*, **81**, 2328 (1989)

7. Van De Nesse, R. J., Hoogland, G. J. M., DeMoel, J. J. M., Gooijer, C., Brinkman, U. A. Th., Velthorst, N. H. *J. Chrom.*, **552**, 613 (1991)

8. Kashawneh, I. M., Chamsez, M., Winefordner, J. D. *Anal. Lett.*, **21**, 125 (1988)

9. Cline Love, L. J., Skrilec, M., Habarta, J G. *Anal. Chem.*, **52** 754 (1980)

10. Plakhotnik T. V., Personov, R. I., Gastilovich, E. A. *J. Chem. Phys.*, **150**, 429 (1991)

11. Gooijer, C. Ariese, I., Velthorst, N. H., Hofstraat, J. W. *Anal. Chim. Acta*, **232** 245 (1990)

12. Hofstraat, J. W. Gooijer, C., Velthorst, N. H. *Appl.Spec.*, **42**, 614 (1988)

13. Jankowiak R., Small. G. *Anal. Chem.*, **61** 1023A (1989)

14. Personov. R. I. "Site Selection Spectroscopy of Complex Molecules and Its Applications "V. M. Agranovich and R. M. Hochstrasser, Eds., North-Holland Publishing Co. Amsterdam (1983)

15. Hayes, J. M., Small, G. J. *Anal. Chem.*, **55** 565A (1983)

16 Goates, S. R.; Lee, M. L. **DOE/PC/90534-15**, U. S. Government, Washington, DC (1989)

17. Staller, S. W.; Johnston, M. V. *Anal. Chem.*, **59**, 567 (1987)

18 MacDonald, B. F.; Hammons, J. L.; Gore, R. R.; Maple, J. R.; Wehry, E. L. *Appl. Spec.*, **42**, 1079 (1988)

19 Weeks, S. J.; Gilles, S. M.; D'Silva, A. P. *Appl. Spec.*, **45**, 1093 (1991)

20 Shpol'skii, E. V. *Usp. Fiz. Nauk*, **71**, 215 (1960)

21. Rima, J.; Rizk, T. J.; Garrigues, P.; Lamotte, M. *Polycyclic Aromatic Compounds*, **1**, 161 (1990)

22 Lai, E. P.; Inman, E. L.; Winefordner, J. D. *Talanta*, **29**, 601 (1982)

23. Maple, S. I.; Wehry, E. L. *Anal. Chem.*, **53**, 266 (1981)

24 Colmsjo, A.; Zebuhr, Y.; Ostman, C. *Chemica Scripta*, **24**, 95 (1984)

25 Yang, Y.; D'Silva, A. P.; Fassel, V. A. *Anal. Chem.*, **53**, 894 (1981)

26. Jacob, J.; Karcher, W.; Belliardo, J. J.; Dumler, R. *Fres. J. Anal. Chem.*, **340**, 755 (1991)

27 Colmsjo, A.; Ostman, C. E. "Atlas of Shpol'skii Spectroscopy," University of Stockholm Press, Stockholm (1981)

28 Garrigues, P.; Bellocq, J.; Wise, S. A. *Fres. J. Anal. Chem.*, **336**, 106 (1990)

29 Jones, B. T.; Winefordner, J. D. *Anal. Chem.*, **60**, 412 (1988)

30 Colmsjo, A.; Ostman, C. E. *Anal. Chim. Acta*, **208**, 183 (1988)

31 Maple, J. R.; Wehry, E. L.; Mamantov, G. *Anal. Chem.*, **52**, 920 (1980)

32 Bourne, S.; Haefner, A. M.; Norton, K. L.; Griffiths, P. R. *Anal. Chem.*, **62**, 2448 (1990)

33 Clos, J. F. "A Self-Cleaning, Low-Temperature Molecular Luminescence Spectrometer as a Detector for Gas Chromatography," Ph. D. Dissertation, University of Florida, Gainesville, (1988)

34 Imasaka, T , Fukuoka, H , Hayashi, T , Ishibashi, N *Anal. Chim. Acta*, **156**, 111 (1984)

35 Giddings, J C *Anal Chem* , **34**, 314 (1962)

36 Puig, L., Sacks, R D *J Chrom Sci* , **23**, 158 (1991)

37 Hail, M E , Yost, R A *Anal. Chem* , **61**, 2402 (1989)

38 Berner, U "Short Column Gas Chromatograhy with Flame Ionization Detection Under Vacuum Outlet Conditions," Master's Thesis, University of Florida Gainesville, (1992)

39 Hyver, K J , Phillips, R J *J Chrom* , **399**, 33 (1987)

40 Trehy, M L , Yost, R A , Dorsey, J G *Anal Chem* , **58**, 12 (1986)

41 Ettre, L. S *Chromatographia* **18** 243 (1984)

42 Leclercq P A , Cramers, C A *J High Res Chrom & Chrom. Comm* , **8**, 764 (1985)

43 Leclercq P A , Cramers, C A *J High Res Chrom. & Chrom Comm* , **10**, 269 (1987)

44 Shoemaker, D P Garland, C W Steinfeld, J I , Nibler, J N "Experiments in Physical Chemistry," Fourth Ed , McGraw-Hill Book Company New York (1981)

45 McNair, H M Bonelli E J "Basic Gas Chromatography," Varian Aerograph Walnut Creek, CA (1968)

46. Brown, R S , Wilkins, C L *Anal Chem* **60**, 1483 (1988)

47 Craddock, S , Hinchcliffe, A J "Matrix Isolation," Cambridge University Press London England (1975)

48 Inman, E L. "Total Luminescence Spectroscopy for Selectivity Enhancement in Multicomponent Analysis," Ph D Dissertation, University of Florida, Gainesville (1982)

49 Azumi, T., McGlynn, S P *J Chem Phys* **41**, 3131 (1964)

50 Jones, B T , Mullins N J , Winefordner, J D *Anal Chem.*, **61**, 1182 (1989)

51 Azumi, T , McGlynn, S P *J Chem Phys* , **39** 1186 (1963)

52 Azumi, T , McGlynn, S P *J Chem. Phys* , **38**, 1016 (1963)

53 Porro, T J , Anacreon, R. E., Flandreau, P S , Fagerson, J S *J of the AOAC*, **56**, 607 (1973)

54 Parker, C A , Hatchard, C G *Analyst*, **87**, 664, (1962)

55 Barnard, T W , Crockett, M I , Ivalds, J C , Lundberg, P L *Anal. Chem.*, **65**, 1225 (1993)

56 Barnard T W , Crockett, M I , Ivalds, J C Lundberg, P L , Yates, D A , Levine, P A , Sauer, D J , *Anal Chem* , **65**, 1231 (1993)

BIOGRAPHICAL SKETCH

Nancy Jean Mullins was born on March 1, 1965 in Anna Maria, Florida. She received her A.A. from Manatee Community College in May, 1986. During this time she worked at Mote Marine Laboratory in Sarasota, Florida, in the laboratory of Dr. Seymour Zigman of the University of Rochester Medical School. This research was in the study of chemical changes which occur to lens proteins during the formation of cataracts. She received her B.S. in chemistry from the University of Florida in 1988, where she performed undergraduate research in the laboratory of J. D. Winefordner studying low temperature molecular luminescence. She currently is a professor of chemistry at Florida Community College at Jacksonville, and attends the University of Florida from which she plans to receive her Doctor of Philosophy degree in analytical chemistry.

I certify that I have read this study and that in my opinion it conforms to acceptable standards of scholarly presentation and is fully adequate, in scope and quality, as a dissertation for the degree of Doctor of Philosophy

James D. Winefordner

James D Winefordner, Chairman
Graduate Research Professor
of Chemistry

I certify that I have read this study and that in my opinion it conforms to acceptable standards of scholarly presentation and is fully adequate, in scope and quality, as a dissertation for the degree of Doctor of Philosophy

Eric R Allen
Professor of Environmental
Engineering Sciences

I certify that I have read this study and that in my opinion it conforms to acceptable standards of scholarly presentation and is fully adequate, in scope and quality, as a dissertation for the degree of Doctor of Philosophy

David R Powell
Associate Scientist of
Chemistry

I certify that I have read this study and that in my opinion it conforms to acceptable standards of scholarly presentation and is fully adequate, in scope and quality, as a dissertation for the degree of Doctor of Philosophy

Martin T. Vala

Martin T Vala
Graduate Research Professor
of Chemistry

I certify that I have read this study and that in my opinion it conforms to acceptable standards of scholarly presentation and is fully adequate, in scope and quality, as a dissertation for the degree of Doctor of Philosophy

Vaneica Young

Vaneica Y Young
Associate Professor of
Chemistry

This dissertation was submitted to the Graduate Faculty of the Department of Chemistry in the College of Liberal Arts and Sciences and to the Graduate School and was accepted as partial fulfillment of the requirements for the degree of Doctor of Philosophy

April, 1994

Dean, Graduate School